Supplemental Information for

Expanded Kinetic Control for Persistent Micelle Templates with Solvent Selection

Amrita Sarkar[†], Laurel Evans[‡] and Morgan Stefik[†*]

[†] Department of Chemistry and Biochemistry, University of South Carolina, Columbia, South Carolina 29208, United States

[‡]Present Address: Spring Valley High School, 120 Sparkleberry Ln, Columbia, South Carolina 29229, United States

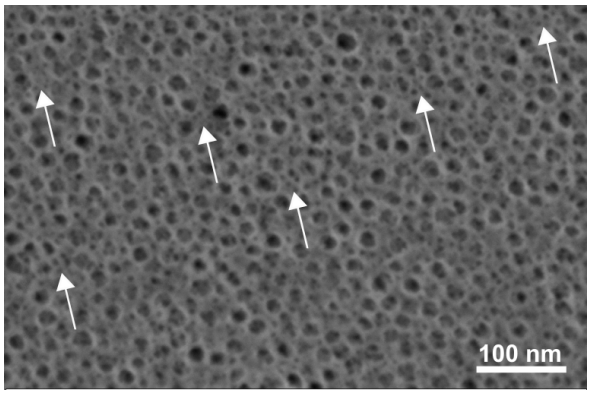

Figure S1. SEM of film made using PEO-*b*-PHA diblock copolymer (12.7 kgmol^{-1}, Đ = 1.10) with 17w% water and M:T=1.50. The primary pores (12.50±0.218 nm) are accompanied by secondary porosity indicated with arrows (4.57±0.133 nm).

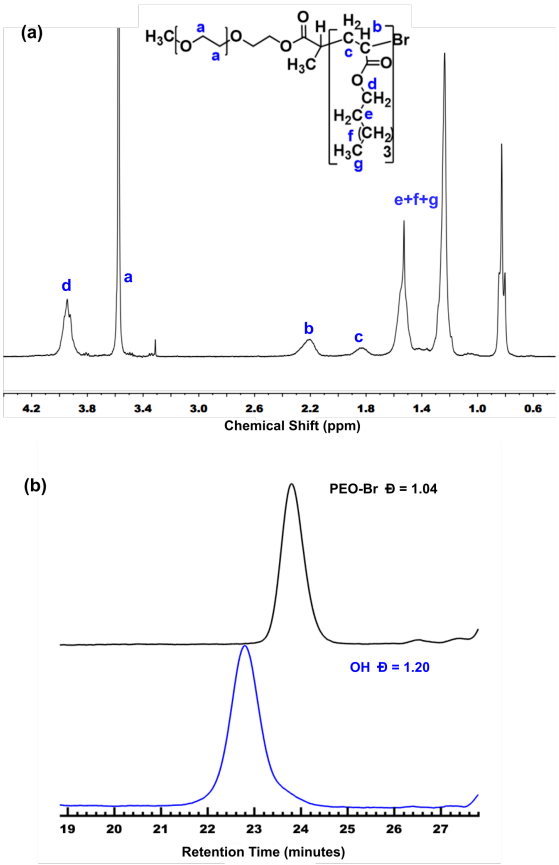

Figure S2. ^{1}H NMR (a), and GPC (b) of **OH** diblock copolymer demonstrating controlled chain extension with narrow molar mass dispersity.

Derivation of Log-Log Coordinate Space for Validation of SAXS Consistency with PMT Lattice Expansion:

A relationship was previously derived[26] to predict micelle template or pore size based upon SAXS measurements using a simple lattice model and a conservation of volume argument. There the micelle template radius r scaled with:

$$r = Cd^* \left(x\beta_{mct} + 1 + \frac{f_{corona}}{1 - f_{corona}} \right)^{-1/3} \quad \text{(eq S1)}$$

where the constant C had specific values depending on symmetry, or lack thereof in the paracrystalline case. Here d* is the d-spacing corresponding to the first SAXS structure factor peak, x is the material:template ratio, and f_{corona} is the volume fraction of the corona block. Rearranging (eq S1) to solve for d* results in:

$$d^* = \frac{r}{C} \left(x\beta_{mct} + 1 + \frac{f_{corona}}{1 - f_{corona}} \right)^{1/3} \quad \text{(eq S2)}$$

Taking the log of both sides and simplifying results in:

$$log(d^*) = log(\frac{r}{C}) + \frac{1}{3} log \left(x\beta_{mct} + 1 + \frac{f_{corona}}{1 - f_{corona}} \right) \quad \text{(eq S3)}$$

The resulting equation provides a simple linear relationship on a log-log plot of d* vs a term with x. However, the β_{mct} in this term is an experimental fit parameter that is rarely known apriori. Since 3>x>1, β_{mct} >~4 and f_{corona} <0.4 so one may approximate that:

$$x\beta_{mct} + 1 + \frac{f_{corona}}{1 - f_{corona}} \approx x\beta_{mct} \quad \text{(eq S4)}$$

This approximation allows (eq S3) to be approximated as:

$$log(d^*) \approx log(\frac{r}{C}) + \frac{1}{3} log\,(x\beta_{mct}) = log(\frac{r}{C}) + \frac{1}{3} log(\beta_{mct}) + \frac{1}{3} log(x) \quad \text{(eq S5)}$$

Here the kinetic entrapment of persistent micelle conditions would maintain constant radius r where the lattice expansion of d* is a result of increasing the wall-thickness alone. Under these conditions a log-log plot of d* vs x should be approximately a straight line with slope of 1/3. This relationship provides considerable utility for fitting where the fit region may be constrained based upon intrinsic scaling relationships for d* to x based on this simple scaling relationship.

Table S1. Time resolved DLS measurements of micelles in MeOH-HCl(aq) solution as a function of quiescent sit time.

Quiescent Time (min)	Mean Hydrodynamic Diameter ± Standard Deviation (nm)
0	**35±7**
15	**35±7**
30	**35±7**
60	**35±7**
120	**35±7**
180	**35±7**
480	**36±7**

All data were measured at 25 ºC. The refractive index and viscosities of 1.326 and 0.607 cP, respectively, were used for the mixture.

Table S2. DLS measurements **OH** micelles in MeOH-water with constant 1.96 vol% water and variable HCl content.

wt% HCl	Mean Hydrodynamic Diameter ± Standard Deviation (nm)
0	**18±4**
0.01	**19±4**
0.05	**21±5**
0.12	**23±5**
0.22	**25±5**
0.30	**27±5**
0.38	**27±6**

Micelles were prepared in MeOH and DI water. Next a stock solution of 0.5M methanolic HCl and DI water was added dropwise (matched vol% water to the micelle solution). The resulting mixture maintained constant water composition and variable HCl concentration. DLS was measured at 25 ºC. The mixture refractive index and viscosity used for analysis were 1.326 and 0.607 cP, respectively.

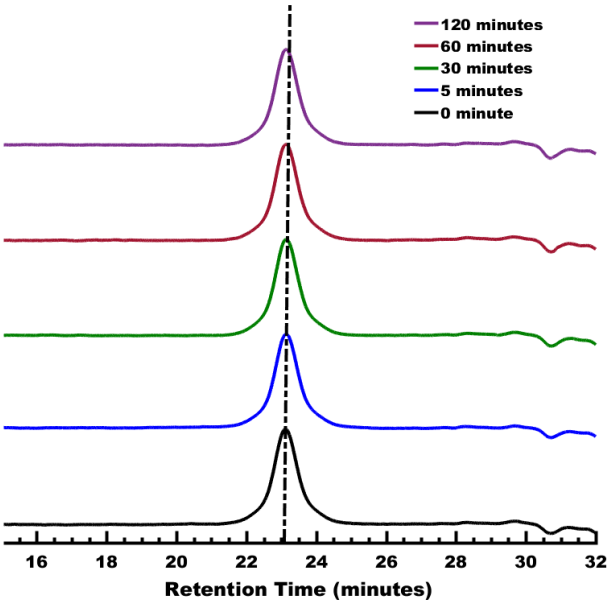

Figure S3. GPC of **OH** as a function of sonication time. There was no detectable change to the molar mass nor the molar mass dispersity (Đ =1.20).

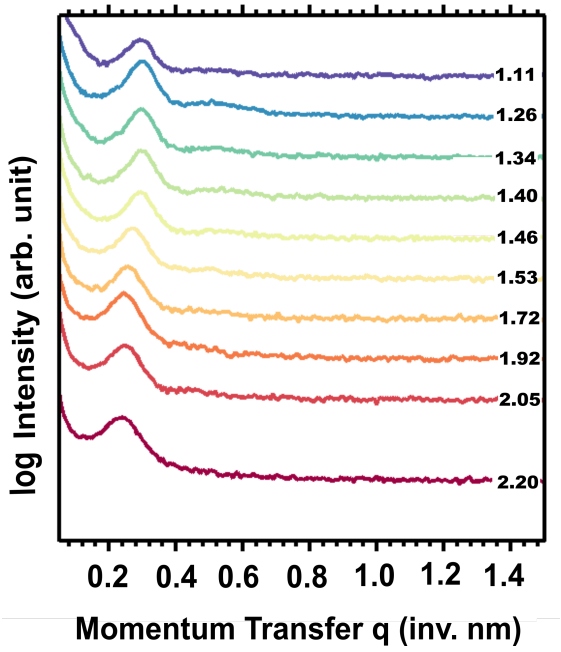

Figure S4. SAXS measurements of **OH-THF-Series1** with increasing Material:Template ratio. The scattering data were offset vertically for clarity.

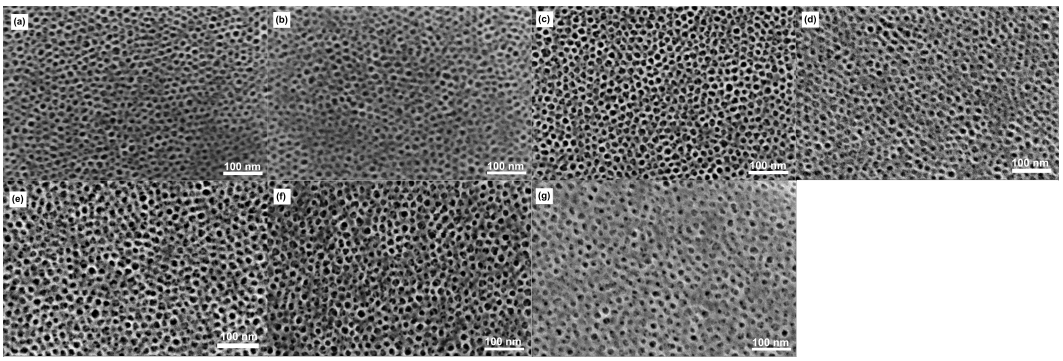

Figure S5. SEM images of **OH-THF-Series1** after calcination. The Material:Template ratios are **1.26** (a), **1.34** (b), **1.40** (c), **1.46** (d), **1.53** (e), **1.63** (f) and **1.92** (g).

Table S3. Measurements of **OH-THF-Series**

Sample	M:T ratio	SAXS d-spacing (nm)	SEM average pore diameter (nm)	SEM average wall thickness (nm)	Wall:Pore ratio (unitless)
OH-THF-series1-1.26	1.26	20.91±1.40	12.88±0.191	6.02±0.194	0.47
OH-THF-series1-1.34	1.34	21.12±0.34	12.16±0.119	6.29±0.169	0.52
OH-THF-series1-1.40	1.40	21.39±0.81	12.65±0.197	6.61±0.294	0.52
OH-THF-series1-1.46	1.46	21.42±0.23	12.47±0.187	6.60±0.308	0.53
OH-THF-series1-1.53	1.53	22.45±0.68	11.64±0.185	6.70±0.169	0.58
OH-THF-series1-1.64	1.63	23.82±1.52	11.42±0.236	7.58±0.247	0.66
OH-THF-series1-1.72	1.72	24.50±1.94	11.87±0.209	9.59±0.208	0.81
OH-THF-series1-1.83	1.83	24.86±1.21	--	--	--
OH-THF-series1-1.92	1.92	25.51±0.62	12.13±0.193	8.18±0.329	0.67
OH-THF-series1-2.05	2.05	25.90±0.97	11.57±0.21	9.14±0.369	0.79
OH-THF-series2-1.26	1.26	20.87	--	--	--
OH-THF-series2-1.40	1.40	21.06	--	--	--
OH-THF-series2-1.53	1.53	22.22	--	--	--
OH-THF-series2-1.63	1.63	21.65	--	--	--
OH-THF-series2-1.72	1.72	25.11	--	--	--
OH-THF-series3-1.30	1.30	20.15	--	--	--
OH-THF-series3-1.39	1.39	20.48	--	--	--
OH-THF-series3-1.46	1.46	20.78	--	--	--
OH-THF-series3-1.53	1.53	21.12	--	--	--
OH-THF-series3-1.60	1.60	20.34	--	--	--
OH-THF-series3-1.64	1.64	20.59	--	--	--
OH-THF-series3-1.77	1.77	22.27	--	--	--
OH-THF-series3-1.87	1.87	24.25	--	--	--
OH-THF-series3-1.95	1.95	29.51	--	--	--
OH-THF-series3-2.01	2.01	23.16	--	--	--

Table S4. Measurements of **OH-EtOH-Series.**

Sample	M:T ratio	SAXS d-spacing (nm)	SEm average pore diameter (nm)	SEM average wall-thickness (nm)	Wall:Pore ratio (unitless)
OH-EtOH-series1-1.29	1.29	19.85±0.174	11.97±0.207	5.86±0.248	0.49
OH-EtOH-series1-1.36	1.36	19.74±0.161	11.64±0.107	7.04±0.185	0.60
OH-EtOH-series1-1.44	1.44	20.01±0.078	11.79±0.156	6.08±0.194	0.52
OH-EtOH-series1-1.53	1.53	20.42±0.141	11.75±0.156	6.58±0.159	0.56
OH-EtOH-series1-1.58	1.58	20.61±0.198	--	--	--
OH-EtOH-series1-1.64	1.64	21.03±0.27	11.71±0.164	6.74±0.133	0.58
OH-EtOH-series1-1.71	1.71	21.31±0.18	12.02±0.179	6.81±0.188	0.57
OH-EtOH-series1-1.85	1.85	21.69±0.149	12.03±0.184	7.18±0.177	0.60
OH-EtOH-series1-1.97	1.97	22.67±0.163	12.00±0.232	7.10±0.270	0.59
OH-EtOH-series1-2.06	2.06	23.13±0.171	10.43±0.175	5.83±0.255	0.56
OH-EtOH-series1-2.29	2.29	24.29±0.344	12.14±0.168	7.23±0.253	0.60
OH-EtOH-series1-2.39	2.39	25.19±0.156	11.45±0.162	8.16±0.267	0.71
OH-EtOH-series1-2.51	2.51	28.20±0.352	12.23±0.185	8.28±0.346	0.68
OH-EtOH-series2-1.52	1.52	20.42	--	--	--
OH-EtOH-series2-1.64	1.64	20.94	--	--	--
OH-EtOH-series2-1.75	1.75	21.70	--	--	--
OH-EtOH-series2-1.95	1.95	21.94	--	--	--
OH-EtOH-series2-2.05	2.05	22.52	--	--	--
OH-EtOH-series2-2.11	2.11	22.77	11.41±0.187	6.06±0.282	0.53
OH-EtOH-series2-2.25	2.25	22.59	--	--	--
OH-EtOH-series2-2.37	2.37	23.69	--	--	--
OH-EtOH-series2-2.46	2.46	25.00	--	--	--

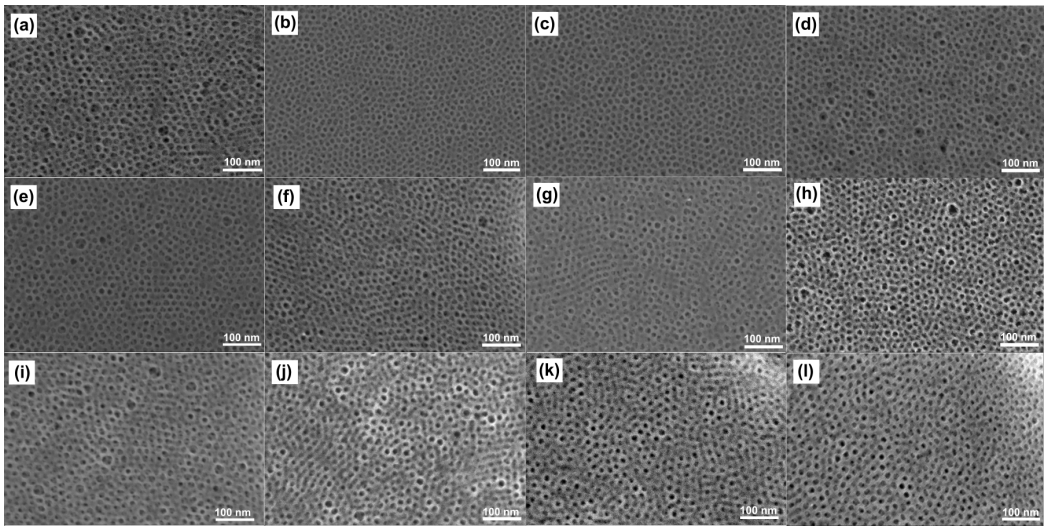

Figure S6. SEM images of **OH-EtOH-Series1** in order of increasing Material:Template ratio: **1.29** (a), **1.36** (b), **1.44** (c), **1.53** (d), **1.64** (e), **1.71** (f) **1.85** (g), **1.97** (h), **2.06** (i), **2.29** (j), **2.39** (k), and **2.51** (l).

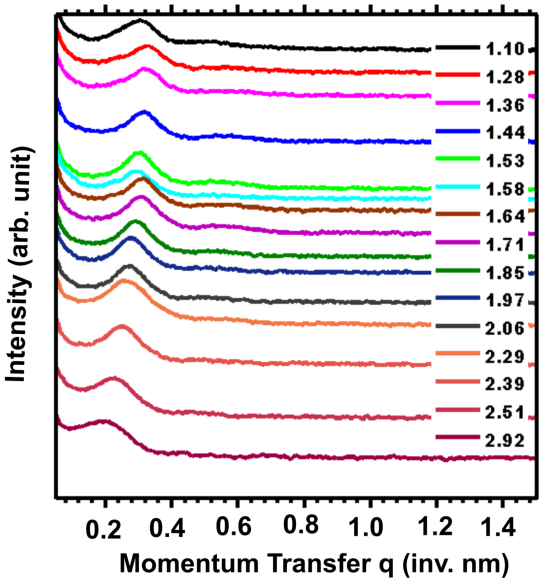

Figure S7. SAXS of **OH-EtOH-Series1** with the increasing Material:Template ratio. The scattering data were offset vertically for clarity.

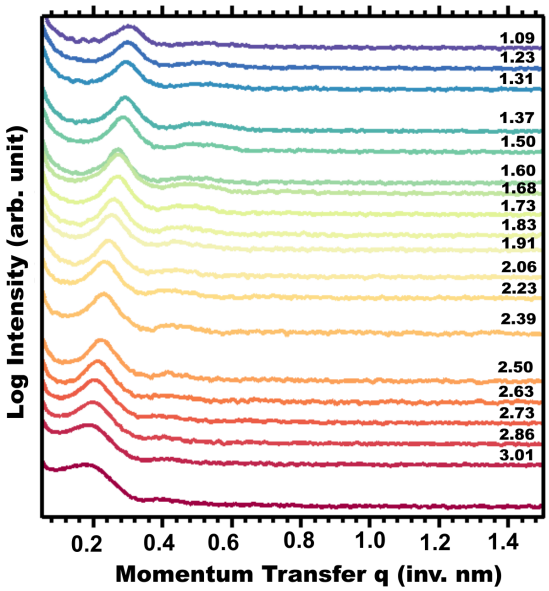

Figure S8. SAXS of **OH-MeOH-Series1** with increasing Material:Template ratio. The scattering data in (a) were offset vertically for clarity.

Table S5. Measurements of **OH-MeOH-Series** samples

Sample	M:T ratio	SAXS d-spacing (nm)	SEM average pore diameter (nm)	SEM average wall-thickness (nm)	Wall:Pore ratio (unitless)
OH-MeOH-series1-1.23	1.23	21.09±0.23	12.75±0.174	6.24±0.194	0.49
OH-MeOH-series1-1.31	1.31	21.44±0.11	--	--	--
OH-MeOH-series1-1.37	1.37	21.67±0.13	--	--	--
OH-MeOH-series1-1.50	1.50	22.14±0.13	12.95±0.234	7.44±0.213	0.57
OH-MeOH-series1-1.60	1.60	22.72±0.30	13.02±0.178	7.80±0.312	0.60
OH-MeOH-series1-1.68	1.68	23.05±0.12	13.29±0.170	8.03±0.282	0.60
OH-MeOH-series1-1.73	1.73	23.54±0.06	13.08±0.176	8.35±0.238	0.64
OH-MeOH-series1-1.83	1.83	24.33±0.12	13.27±0.195	8.58±0.253	0.65
OH-MeOH-series1-1.91	1.91	24.89±0.38	--	--	--
OH-MeOH-series1-2.06	2.06	25.67±0.27	12.75±0.178	9.25±0.366	0.73
OH-MeOH-series1-2.23	2.23	26.97±0.15	13.65±0.139	10.39±0.264	0.76
OH-MeOH-series1-2.28	2.28	27.68	--	--	--
OH-MeOH-series1-2.39	2.39	28.33	14.36±0.193	9.02±0.291	0.63
OH-MeOH-series1-2.50	2.50	29.82	14.10±0.251	12.59±0.400	0.89
OH-MeOH-series1-2.63	2.63	31.16±0.19	14.75±0.166	11.45±0.375	0.78
OH-MeOH-series1-2.73	2.73	32.10±0.25	13.22±0.175	11.26±0.306	0.85
OH-MeOH-series1-2.86	2.86	34.60±0.52	--	--	--
OH-MeOH-series1-3.01	3.01	35.83±0.84	--	--	--
OH-MeOH-series2-1.64	1.64	22.88	--	--	--
OH-MeOH-series2-1.77	1.77	23.44	--	--	--
OH-MeOH-series2-1.85	1.85	23.95	--	--	--
OH-MeOH-series2-1.93	1.93	24.02	--	--	--
OH-MeOH-series2-2.01	2.01	24.57	--	--	--
OH-MeOH-series2-2.10	2.10	25.23	--	--	--
OH-MeOH-series2-2.16	2.16	25.55	12.44±0.142	9.33±0.194	0.75
OH-MeOH-series2-2.26	2.26	25.79	--	--	--
OH-MeOH-series2-2.34	2.34	26.52	--	--	--
OH-MeOH-series2-2.47	2.47	28.00	--	--	--
OH-MeOH-series2-2.59	2.59	29.43	--	--	--
OH-MeOH-series2-2.68	2.68	29.60	--	--	--
OH-MeOH-series2-2.79	2.79	30.74	--	--	--
OH-MeOH-series2-2.94	2.94	32.26	--	--	--
OH-MeOH-series3-1.12	1.12	21.22	--	--	--
OH-MeOH-series3-1.24	1.24	22.23	--	--	--
OH-MeOH-series3-1.32	1.32	21.85	--	--	--
OH-MeOH-series3-1.41	1.41	22.25	--	--	--
OH-MeOH-series3-1.46	1.46	22.73	--	--	--
OH-MeOH-series3-1.55	1.55	23.18	--	--	--
OH-MeOH-series3-1.63	1.63	23.52	--	--	--
OH-MeOH-series3-1.73	1.73	24.08	--	--	--
OH-MeOH-series3-1.83	1.83	24.52	--	--	--
OH-MeOH-series3-1.90	1.90	24.84	--	--	--
OH-MeOH-series3-2.09	2.09	26.02	--	--	--
OH-MeOH-series3-2.24	2.24	27.20	--	--	--
OH-MeOH-series3-2.34	2.34	27.32	--	--	--
OH-MeOH-series3-2.44	2.44	28.68	--	--	--
OH-MeOH-series3-2.50	2.50	30.08	--	--	--
OH-MeOH-series3-2.62	2.62	30.56	--	--	--
OH-MeOH-series3-2.74	2.74	32.73	--	--	--
OH-MeOH-series3-2.89	2.89	34.63	--	--	--
OH-MeOH-series3-3.05	3.05	36.90	--	--	--